Journal of Thrombosis and Haemostasis, **7**: 1886–1896 DOI: 10.1111/j.1538-7836.2009.03606.x

ORIGINAL ARTICLE

Endothelial cell specific adhesion molecule (ESAM) localizes to platelet–platelet contacts and regulates thrombus formation *in vivo*

T. J. STALKER,* J. WU,* A. MORGANS,* E. A. TRAXLER,* L.WANG,* M. S. CHATTERJEE,† D. LEE,‡ T. QUERTERMOUS,§ R. A. HALL,¶ D. A. HAMMER,‡ S. L. DIAMOND† and L. F. BRASS*

*Departments of *Medicine, †Chemical and Biomolecular Engineering, The Institute for Medicine and Engineering, and ‡Bioengineering, University of Pennsylvania, Philadelphia, PA; §Stanford University School of Medicine, Stanford, CA; and ¶Department of Pharmacology, Emory University School of Medicine, Atlanta, GA, USA*

To cite this article: Stalker TJ, Wu J, Morgans A, Traxler EA, Wang L, Chatterjee MS, Lee D, Quertermous T, Hall RA, Hammer DA, Diamond SL, Brass LF. Endothelial cell specific adhesion molecule (ESAM) localizes to platelet–platelet contacts and regulates thrombus formation *in vivo*. *J Thromb Haemost* 2009; **7**: 1886–96.

Summary. *Background:* In resting platelets, endothelial cell specific adhesion molecule (ESAM) is located in alpha granules, increasing its cell surface expression following platelet activation. However, the function of ESAM on platelets is unknown. *Objective:* To determine whether ESAM has a role in thrombus formation. *Methods and results:* We found that following platelet activation ESAM localizes to the junctions between adjacent platelets, suggesting a role for this protein in contact-dependent events that regulate thrombus formation. To test this hypothesis we examined the effect of ESAM deletion on platelet function. *In vivo*, ESAM$^{-/-}$ mice achieved more stable hemostasis than wild-type mice following tail transection, and developed larger thrombi following laser injury of cremaster muscle arterioles. *In vitro*, ESAM$^{-/-}$ platelets aggregated at lower concentrations of G protein-dependent agonists than wild-type platelets, and were more resistant to disaggregation. In contrast, agonist-induced calcium mobilization, $\alpha_{IIb}\beta_3$ activation, alpha-granule secretion and platelet spreading, were normal in ESAM-deficient platelets. To understand the molecular mechanism by which ESAM regulates platelet activity, we utilized a PDZ domain array to identify the scaffold protein NHERF-1 as an ESAM binding protein, and further demonstrated that it associates with ESAM in both resting and activated platelets. *Conclusions:* These findings support a model in which ESAM localizes to platelet contacts following platelet activation in order to limit thrombus growth and stability so that the optimal hemostatic response occurs following vascular injury.

Correspondence: Lawrence F. Brass, University of Pennsylvania, 915 BRB II/III, 421 Curie Blvd, Philadelphia, PA 19104, USA.
Tel.: +1 215–573–3540; fax: +1 215–573–7039.
E-mail: brass@mail.med.upenn.edu

Received 4 February 2009, accepted 12 August 2009

Keywords: ESAM, NHERF-1, PDZ domain, platelets, thrombosis.

Introduction

Thrombus formation *in vivo* is a dynamic process in which vascular injury initiates a cascade of events involving components of the vascular wall, platelets, other blood cells, and plasma proteins. Platelet activation and subsequent aggregation play a critical role in this process, especially in the high shear environment of the arterial circulation. While many of the agonists and receptors responsible for platelet activation have been identified, much less is known about post-aggregation signaling events that regulate thrombus growth and stability so that the optimal hemostatic response occurs. There is, however, ample reason to believe that such mechanisms exist and are essential for normal hemostasis. Several examples of post-aggregation platelet signaling have been described in recent years, including outside-in signaling through the integrin, $\alpha_{IIb}\beta_3$ [1], continuous ADP receptor signaling [2,3], and contact-dependent signaling via platelet surface receptor–ligand interactions [4–7]. Each of these signaling mechanisms has been shown to enhance the stability of platelet aggregates *in vitro* and *in vivo*.

In addition to these signaling molecules, platelets express several immunoglobulin superfamily proteins on their surface known to form homotypic interactions in trans between adjacent cells. Among these are the proteins PECAM-1 and CEACAM1, two immunotyrosine based inhibitory motif (ITIM) containing receptors [8,9]. Both of these proteins have been characterized as negative regulators of platelet function because genetic deletion of either protein results in enhanced thrombus formation *in vivo* [8,9]. Interestingly, platelets also express four members of the CTX family of adhesion molecules, junctional adhesion molecule-A (JAM-A) [10], JAM-C [11], endothelial cell specific adhesion molecule

(ESAM) [12] and DNAM-1 (CD226) [13], which also mediate interactions in trans between adjacent cells. Unlike PECAM-1 and CEACAM1, this family of proteins does not contain ITIM domains in their cytoplasmic tails. Whether these proteins mediate platelet–platelet interactions and/or contribute to post-aggregation signaling events that regulate thrombus growth and stability has not been previously studied.

ESAM, which is the subject of this report, is a 55 kDa type I membrane glycoprotein with two extracellular immunoglobulin domains (one V-type and one C2), a single transmembrane domain and a long cytosolic tail that terminates in a type-I PDZ domain ligand [14]. When originally cloned, ESAM was shown to be expressed specifically by endothelial cells in diverse parts of the circulation [12,14], and by megakaryocytes and platelets [12]. Immunofluorescence studies show that ESAM accumulates at cell junctions in transfected cell lines as well as in endothelial cells, where it co-localizes with tight junction proteins [14,15]. Further, ESAM mediates cell clustering via homophilic interactions when expressed in CHO cells [14].

In light of these findings, ESAM was originally characterized as an adhesion molecule. However, generation of ESAM-deficient mice revealed that loss of ESAM from endothelial cell junctions results in increased junctional stability [16]. These findings suggest that rather than contributing adhesive strength to cell contacts, ESAM has a role in the coordinated destabilization of junctions in response to stimuli. In endothelial cells, this role for ESAM was demonstrated to be important for the transmigration of leukocytes [16]. The function of ESAM on platelets has not been previously examined, although studies have demonstrated that ESAM is stored in alpha granule membranes of resting platelets [17], and accordingly its surface expression increases following platelet activation [12]. In addition, a recent study in zebrafish demonstrated that morpholino-mediated knockdown of ESAM expression results in enhanced thrombus formation following laser injury *in vivo* [18].

In the present study we asked whether ESAM has a role in thrombus formation. The results show that: (i) ESAM concentrates at the junctions between platelets following platelet activation; to our knowledge this is the first demonstration of a cell adhesion molecule localizing to platelet–platelet contacts; (ii) ESAM-deficient mice achieve more stable hemostasis following tail transection and show increased platelet accumulation and fibrin formation following laser injury *in vivo*; (iii) platelets from ESAM-deficient mice aggregate at lower agonist concentrations and the aggregates that form are more stable than wild-type platelets; and (iv) fibrin clot retraction is delayed in the absence of ESAM. Taken together, these findings suggest that following platelet activation, ESAM localizes to areas of platelet–platelet contact in order to limit the extent of thrombus formation following vascular injury. To identify the molecular mechanism by which ESAM regulates platelet function we performed a PDZ-domain library screen and identified a scaffold protein, NHERF-1, that interacts with the ESAM cytoplasmic tail *in vitro* and associates with ESAM in platelets.

Methods

ESAM$^{-/-}$ mice

The generation of ESAM-deficient mice was described previously [19]. They have been backcrossed on to a C57Bl/6 background for five generations. Mice used for the current studies (ESAM$^{+/+}$ and $^{-/-}$) were generated from homozygous crosses of parents obtained from heterozygous crosses. The Institutional Animal Care and Use Committee (IACUC) of the University of Pennsylvania approved all mouse studies.

Platelet preparation

Human platelets Whole blood was drawn from healthy volunteers according to the University of Pennsylvania Institutional Review Board guidelines, using ACD (65 mM trisodium citrate, 70 mM citric acid, 100 mM dextrose, pH 6.5) as the anticoagulant. Following centrifugation at 150 *g* to obtain platelet-rich plasma, the platelets were gel filtered over Sepharose 2B in a modified Tyrode's buffer (4 mM HEPES, pH 7.4, 135 mM NaCl, 2.7 mM KCl, 3.3 mM NaH_2PO_4, 2.4 mM $MgCl_2$, 0.1% glucose and 0.1% BSA).

Mouse platelets Following anesthesia (90 mg kg^{-1} pentobarbital i.p.), mouse blood was drawn via cardiac puncture using heparin as the anticoagulant. The blood was diluted with an equal volume of Tyrode's buffer and centrifuged at 150 *g* to obtain platelet-rich plasma. Platelet counts were normalized to 2.5×10^8 platelets mL^{-1} using Tyrode's buffer.

Immunofluorescence Human gel-filtered platelets were activated with the PAR-1 agonist SFLLRN (10 μM) on microscope slides coated with 100 μg mL^{-1} fibrinogen for 25 min at 37 °C. The platelets were then fixed (3.7% formaldehyde), permeabilized (0.2% Triton X-100), and blocked in 5% BSA followed by application of either anti-ESAM antiserum or rabbit pre-immune serum. The ESAM antiserum was generated using the ESAM extracellular domain (a.a. 30–248) as the immunogen (Covance Research Products, Denver, PA, USA). FITC-conjugated goat anti-rabbit antibody (Jackson Immunoresearch, West Grove, PA, USA) was used as a secondary reagent. Slides were visualized by confocal microscopy using a Zeiss LSM510 confocal microscope system (Carl Zeiss Microimaging, Inc. Thornwood, NY, USA).

Platelet aggregation Mouse platelet aggregation was performed as previously described using an optical aggregometer (Chronolog, Haverford, PA, USA) [20]. The PAR-4 agonist peptide AYPGQV (synthesized by Biopeptide, San Diego, CA, USA), ADP (Sigma, St. Louis, MO, USA) and collagen (Chronolog) were used to stimulate platelet aggregation. In a separate set of experiments, platelets were

induced to disaggregate by adding either apyrase (Sigma) or the $\alpha_{IIb}\beta_3$ antagonist tirofiban (Medicure, Winnipeg, Canada) following peak aggregation in response to ADP.

Bleeding time Following anesthesia with 90 mg kg^{-1} pentobarbital, 5 mm of the mouse tail was cut and the tail submerged in warm saline. The time until bleeding stopped for at least 10 s was recorded. The tail continued to be observed for up to 10 min, and the number of mice that began rebleeding from the tail wound was also recorded, as was the time until rebleeding occurred.

Laser-induced thrombus formation in mouse cremaster muscle arterioles Thrombus formation was visualized in the cremaster muscle microcirculation of male wild-type and $ESAM^{-/-}$ mice according to procedures developed by Falati *et al.* [21]. Alexa-488-labeled anti-α_{IIb} antibody $F(ab)_2$ fragments (MWReg30, 240 μg kg^{-1}; BD Bioscience, San Jose, CA, USA) and Alexa-647-labeled anti-fibrin antibodies (clone 59D8) [22] were administered via a catheter in the jugular vein to label platelets and fibrin, respectively. Arterioles of 30–50 μm in diameter were selected for study, and vascular injury was induced using a pulsed nitrogen dye laser fired through the microscope objective. Brightfield and fluorescent images were captured using a digital CCD camera (SensiCam, Cooke, Auburn Hills, MI, USA) coupled to Slidebook 4.2 image acquisition software (Intelligent Imaging Innovations, Denver, CO, USA). Up to 10 injuries were made in each mouse and three mice were studied in each group. Data are reported as the background-subtracted median integrated fluorescence intensity. Statistical analysis was performed using the Mann–Whitney test.

To determine the contribution of platelet ESAM vs. endothelial cell ESAM to thrombus formation using this model, we generated radiation chimera mice. Fetal liver cells were isolated from 16 to 18 d.p.c. wild-type or $ESAM^{-/-}$ fetuses and injected retro-orbitally into lethally irradiated male wild-type recipients (Cesium-137, 10 Gy, Gammacell 40 Exactor; MDS Nordion, Ontario, Canada). Intravital microscopy experiments were performed as described above 4 weeks after transplant. Hematopoietic reconstitution was confirmed by measuring platelet counts prior to intravital experiments.

Flow cytometric analysis of mouse platelets Mouse PRP was diluted in Tyrode's buffer to obtain a platelet concentration of 1×10^7 platelets mL^{-1}. Either FITC-labeled fibrinogen (100 μg mL^{-1}; Invitrogen, Carlsbad, CA, USA), FITC-anti-α_{IIb} (MWReg30; BD Bioscience), FITC-anti-GPIb (Xia.G5; Emfret Analytics, Eibelstadt, Germany), FITC-anti-JAM-A (Jul.E1; Emfret), FITC-anti-P-selectin (Wug.E9; Emfret) or a phycoerythrin-labeled antibody that recognizes only the active conformation of $\alpha_{IIb}\beta_3$ (JON/A; Emfret) were added to 100 μL (10^6 platelets) of the diluted PRP from either wild-type or $ESAM^{-/-}$ mice. Platelets were incubated with or without the PAR4 agonist peptide AYPGKF (200 μM; Bachem, Torrance, CA, USA) for 5 min at 37 °C, diluted 5-fold in PBS and immediately analyzed using a FACSort flow cytometer (BD Bioscience).

Platelet calcium mobilization Washed mouse platelets pooled from two mice were loaded with Fura-2 (25 μg; Invitrogen) for 45 min at room temperature, followed by an additional wash in HEN buffer (10 mM HEPES, 150 mM NaCl and 1 mM EDTA, pH 6.5 plus 1 mM PGE_1) and finally resuspended in Tyrode's buffer. An 'agonist plate' containing varying concentrations of platelet agonists was prepared on a Perkin Elmer Janus. Cytosolic calcium flux was measured at excitation 340/380 and emission 510 nm in high-throughput fashion using a Molecular Devices FlexStation (Sunnyvale, CA, USA). The 340/380 fluorescence ratio [$R(t)$] was scaled to the mean baseline value for each well [$R_0(t)$] and relative calcium concentrations were quantified as $R(t)/R_0(t)$. All conditions were tested in replicates of eight.

Platelet spreading Washed $ESAM^{+/+}$ or $^{-/-}$ platelets were stimulated with the PAR-4 agonist peptide AYPGKF (200 μM) and spread on immobilized fibrinogen (100 μg mL^{-1}) on a glass coverslip (No. 1.5). Platelets were visualized by reflection interference contrast microscopy using an inverted microscope (Axiovert 200; Karl Zeiss, Goettingen, Germany) with an antiflex 63 × oil immersion objective and appropriate polarizers. Images were recorded using a charge-coupled device camera (Retiga Exi Fast Cooled Mono 12-bit camera 32-0082B-128, QIMAGING, Burnaby, Canada).

Clot retraction Blood from $ESAM^{+/+}$ or $^{-/-}$ mice was drawn into sodium citrate (0.38% final concentration). Clot formation was induced by the addition of 10 U mL^{-1} thrombin (Haematologic Technologies, Inc., Essex Junction, VT, USA) at 37 °C. Pictures were taken at 15, 30, 45 and 60 min following the addition of thrombin to visualize the extent of clot retraction. Retraction was quantified by determining the two-dimensional area occupied by the clot using Slidebook 4.2 software, and is expressed as the percentage area (clot area/total area*100).

PDZ domain array and co-immunoprecipitation A GST-ESAM fusion protein containing the c-terminal 30 amino acids of ESAM fused to GST was expressed in *E. coli* using the pGEX4λ-T vector (GE Healthcare, Piscataway, NJ, USA), and affinity purified using glutathione sepharose. The GST-ESAM fusion protein was used to probe a PDZ domain array as previously described [23]. Bound GST-ESAM was detected with HRP-conjugated anti-GST antibody. In separate studies, ESAM was immunoprecipitated from human platelet lysates. Gel-filtered platelets were incubated with or without SFLLRN to activate platelets followed by lysis in 1% Triton X-100. Lysates were incubated with anti-ESAM antibody to immunoprecipitate ESAM, and associated proteins were resolved by SDS-PAGE. An immunoblot was performed using an anti-NHERF-1 antibody (BD Biosciences) to demonstrate association of ESAM and NHERF-1 in platelets.

The reverse co-immunoprecipitation was also performed (immunoprecipitate NHERF-1 and blot for ESAM).

Statistical analysis Statistical analysis was performed using a two-tailed Student's *t*-test unless otherwise noted.

Results

Localization of ESAM to platelet contacts

Nasdala *et al.* [12] previously demonstrated that ESAM is expressed on mouse platelets, and that its surface expression increases following platelet activation. We found similar results regarding ESAM expression in human platelets, including increased surface expression following platelet activation (Fig. 1A,B). Immunofluorescence studies demonstrated that ESAM is distributed diffusely on isolated platelets spread on immobilized fibrinogen (Fig. 1C, panels i, ii). Strikingly, when two or more platelets came in contact with each other ESAM became concentrated at the junction between the platelets. To our knowledge, this is the first demonstration of a cell adhesion molecule localizing to platelet–platelet contacts. Increased ESAM surface expression following activation, coupled with localization of ESAM at platelet–platelet contacts, suggests a role for ESAM in contact-dependent regulation of platelet function.

Hemostasis in ESAM$^{-/-}$ mice

ESAM-deficient (ESAM$^{-/-}$) mice were described previously [19]. Initial studies reported that they have normal platelet counts with no profound bleeding abnormalities, but have demonstrable defects in pathologic angiogenesis and leukocyte transmigration [16,19]. To determine whether ESAM has a role in hemostasis *in vivo*, we assessed platelet function in ESAM$^{-/-}$ mice by measuring the tail bleeding time and by observing thrombus formation in the arteriolar microcirculation using intravital microscopy. We found no significant difference in the initial bleeding time between wild-type and ESAM$^{-/-}$ mice (117.5 ± 25.6 and 165.8 ± 35.7 s, respectively; mean ± SEM, $P = 0.13$), but re-bleeding occurred less frequently in the ESAM$^{-/-}$ mice. Our procedure involved cutting the distal 5 mm of the mouse tail, which resulted in only 10% of the tails from wild-type mice remaining stably occluded after 10 min (Fig. 2A). The remainder began re-bleeding 177 ± 29 s (mean ± SEM, $n = 19$) following the initial occlusion. In contrast, 29% of the transected ESAM$^{-/-}$ tails remained stably occluded and the average time until re-bleeding occurred in the remaining mice increased to 284 ± 49 s ($P < 0.05$ vs. WT, $n = 14$), indicating that ESAM$^{-/-}$ mice are more likely to form stable occlusions in this assay.

Real time intravital digital microscopy was used to examine thrombus formation *in vivo* induced by laser injury to mouse cremaster muscle arterioles, as previously described [21]. Arteriolar wall shear rates were comparable in wild-type and ESAM-deficient mice (2116 ± 91 s^{-1}, $n = 26$ and 1884 ± 123 s^{-1}, $n = 25$ for WT and ESAM$^{-/-}$, respectively). We examined both platelet accumulation and fibrin formation following laser injury. The kinetic profile of platelet accumulation was similar in wild-type and ESAM$^{-/-}$ mice, but the thrombi that formed were significantly larger in ESAM$^{-/-}$ mice ($P < 0.05$, Fig. 2B,C). Initial fibrin accumulation was similar in the presence and absence of ESAM, but was significantly increased at later time-points during our observation period (Fig. 2D, $P < 0.05$ after 180 s).

To demonstrate that the observed effect on thrombus formation *in vivo* was not due to the loss of ESAM from endothelial cells, we generated chimeric mice by transplanting fetal liver cells from either wild-type or ESAM-deficient donors into lethally irradiated wild-type recipients. Chimeric mice lacking ESAM on their platelets, but with endothelial cell ESAM expression intact, formed larger thrombi in response to laser injury than chimeric mice that expressed ESAM on their platelets (Fig. 2E). These results confirm that loss of ESAM from platelets is largely responsible for the observed increase in thrombus formation in ESAM-deficient mice using this thrombosis model. Thus, in two different models in which hemostasis was examined *in vivo*, thrombus formation was enhanced in mice lacking ESAM.

ESAM$^{-/-}$ platelet function ex vivo

To determine the mechanism responsible for the enhanced thrombus formation observed in ESAM$^{-/-}$ mice *in vivo*, we examined the aggregation profile of platelets from ESAM-deficient mice *in vitro*. We found that aggregation of platelets lacking ESAM was consistently increased compared with their wild-type counterparts in response to sub-maximal concentrations of collagen, ADP and the PAR-4 agonist peptide, AYPGQV (Fig. 3). This enhanced platelet aggregation was dependent on the integrin $\alpha_{IIb}\beta_3$, as pretreatment of platelets with the $\alpha_{IIb}\beta_3$ antagonist tirofiban completely prevented aggregation of both wild-type and ESAM$^{-/-}$ platelets (data not shown). Notably, the enhanced aggregation in response to collagen was dependent on released ADP and thromboxane A_2, as identical responses to collagen were observed in ESAM$^{-/-}$ and wild-type platelets following pretreatment with aspirin and the $P2Y_{12}$ antagonist cangrelor (data not shown). However, the enhanced platelet aggregation observed with ESAM$^{-/-}$ platelets stimulated with a PAR-4 agonist peptide was apparent even when secondary mediators (ADP and TxA_2) were inhibited (data not shown). Taken together, these results demonstrate that platelets lacking ESAM exhibit enhanced aggregation following stimulation of GPCR-dependent signaling pathways.

Effects on aggregate stability

Because thrombus stability was increased in ESAM$^{-/-}$ mice, we also examined the stability of platelet aggregates in the absence of ESAM. Recent studies have demonstrated that platelet aggregates can be induced to fall apart by interrupting ADP

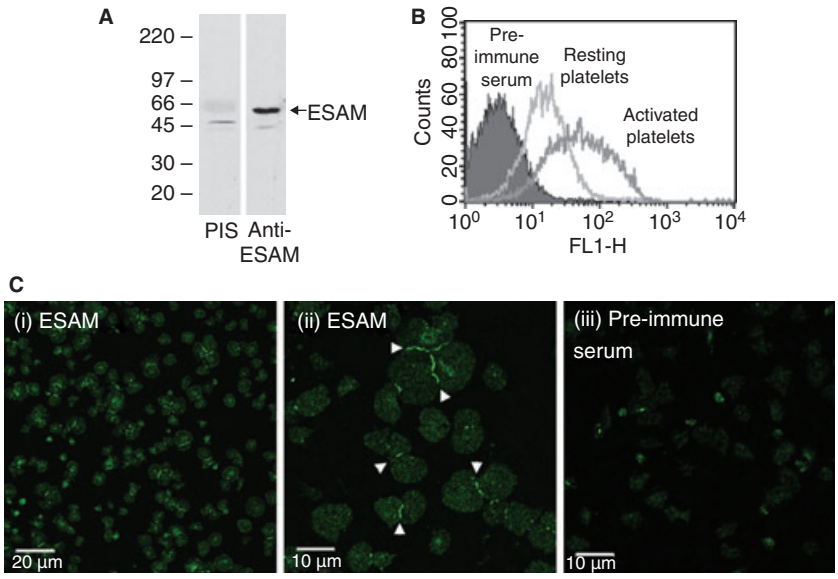

Fig. 1. ESAM localizes to platelet–platelet contacts following platelet activation. (A) Human gel-filtered platelets were lysed and proteins separated by SDS–PAGE. An immunoblot was performed using rabbit anti-ESAM or rabbit pre-immune serum (PIS). (B) Flow cytometric analysis of resting or activated (10 μM SFLLRN) human platelets stained with anti-ESAM or pre-immune serum followed by fluorescently labeled anti-rabbit secondary antibody. (C) Human platelets were activated with 10 μM SFLLRN and allowed to spread on immobilized fibrinogen. The platelets were stained with either rabbit anti-ESAM (panels i and ii) or pre-immune serum (panel iii), as described in Methods. Scale bars: (i) 20 μm, (ii, iii) 10 μm. Arrowheads indicate intense ESAM staining at platelet–platelet contacts. The photomicrographs are representative of at least three independent experiments.

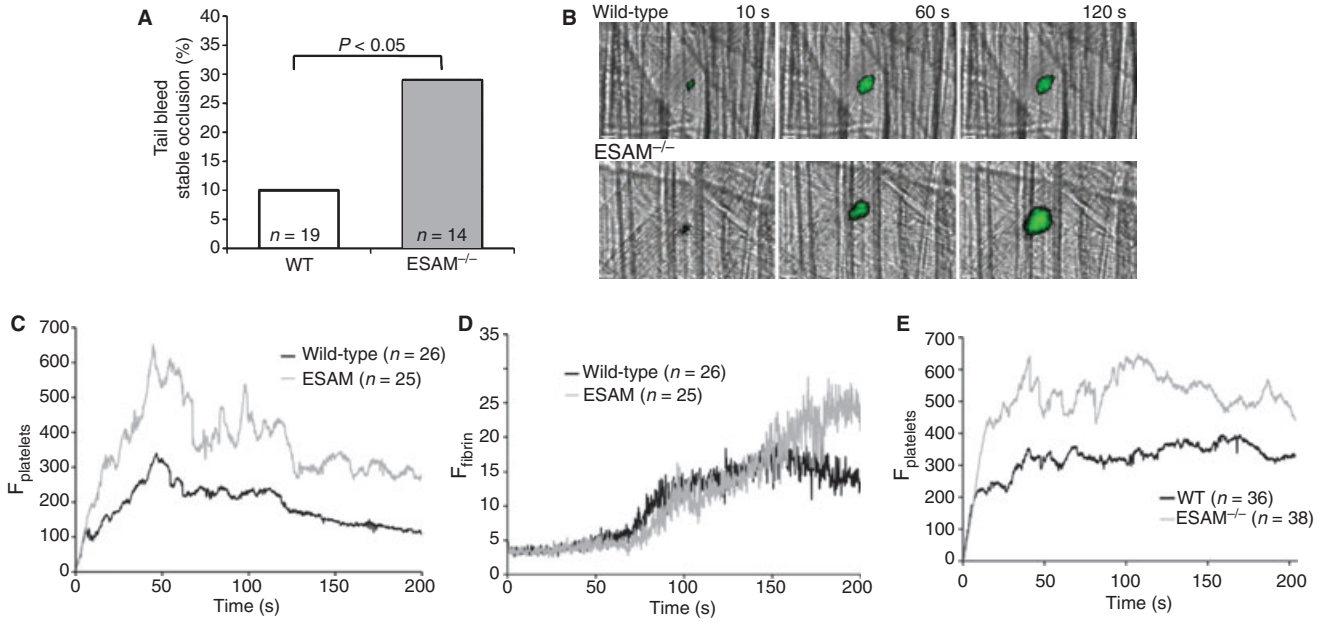

Fig. 2. ESAM-deficient mice form larger, more stable thrombi than wild-type mice *in vivo*. (A) A bleeding time assay was performed by cutting the distal 5 mm of the mouse tail. The percentage of mice that formed stable hemostatic plugs (i.e. did not re-bleed) up to 10 min after initial occlusion is shown. Statistical analysis was performed using Fisher's exact test. (B) Photomicrographs show representative time-lapse images of laser-induced thrombus formation in cremaster muscle arterioles of wild-type and ESAM$^{-/-}$ mice. Platelets are labeled green. (C, D) Median integrated fluorescence intensity is reported (arbitrary units) as a quantitative measure of platelet (C) and fibrin accumulation (D) in cremaster muscle arterioles following laser injury. Statistical analysis was performed using the Mann–Whitney test (n = 26 thrombi from 4 wild-type mice and n = 25 thrombi from 5 ESAM$^{-/-}$ mice). (E) Laser-induced thrombus formation in radiation chimera mice expressing ESAM on their endothelium with or without ESAM expression on their platelets (n = 36 thrombi from 4 mice with wild-type platelets and n = 38 thrombi from four mice with ESAM-deficient platelets).

signaling pathways with a $P2Y_{12}$ receptor antagonist, by hydrolyzing released ADP with apyrase, or by inhibiting the interaction of activated $\alpha_{IIb}\beta_3$ and fibrinogen [2,3]. Using ADP concentrations that resulted in maximum aggregation in both wild-type and ESAM-deficient platelets, we found that ESAM$^{-/-}$ platelet aggregates did not disaggregate to the same

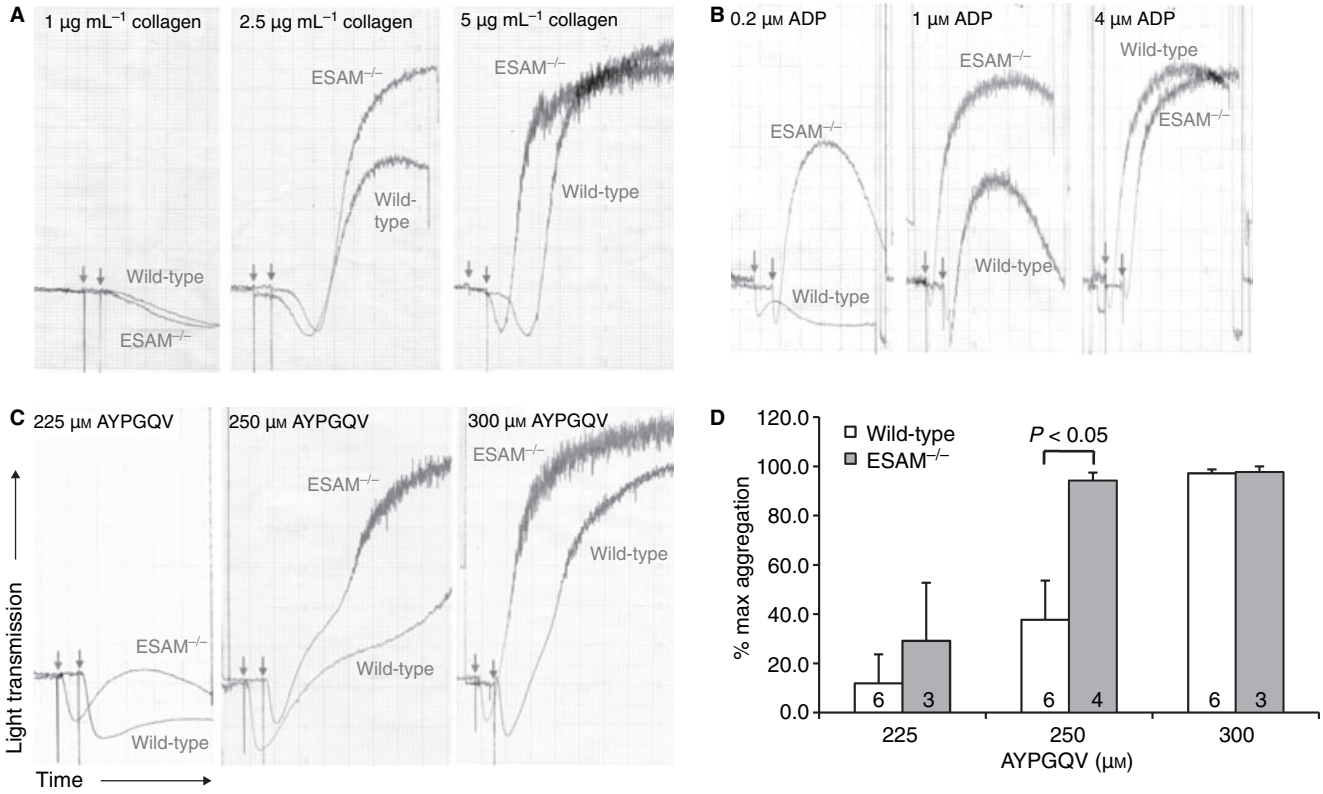

Fig. 3. Lack of ESAM increases platelet aggregation. Platelet aggregation was performed using platelets from wild-type or ESAM$^{-/-}$ mice. (A–C) Representative aggregation tracings for the indicated concentrations of (A) collagen, (B) ADP and (C) the PAR-4 agonist peptide AYPGQV. Arrows indicate addition of agonist. Tracings are representative of at least three independent experiments performed for each condition. (D) Quantitative analysis of aggregation in response to AYPGQV. Data are reported as the extent of aggregation at each agonist concentration normalized to the maximum response in each experiment (max = 100%). Values are mean ± SEM and the numbers at the base of the columns indicate the number of mice in each group.

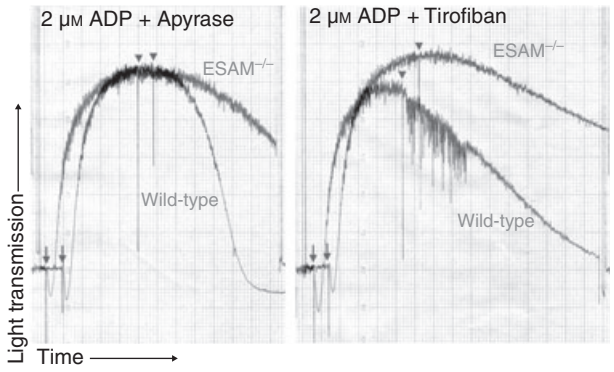

Fig. 4. Lack of ESAM attenuates platelet disaggregation. Platelet aggregation was performed using platelets from wild-type or ESAM$^{-/-}$ mice with ADP (2 μM) as the agonist. Following peak aggregation, either apyrase (0.2 U mL^{-1}, left) or tirofiban (0.5 μM, right) was added to induce disaggregation at the time point indicated by the arrowheads. Arrows indicate addition of ADP.

extent as their wild-type counterparts when apyrase was added following peak aggregation (Fig. 4, left panel). Similar results were obtained with tirofiban, which inhibits fibrinogen binding to $\alpha_{IIb}\beta_3$ (Fig. 4, right panel). In both cases, these data demonstrate that platelets form more stable aggregates in the absence of ESAM.

ESAM$^{-/-}$ platelet surface protein expression

To rule out a role for altered expression of other platelet surface proteins in the observed enhancement in thrombus formation in ESAM$^{-/-}$ mice, we used flow cytometry to measure expression levels of $\alpha_{IIb}\beta_3$, GPIbα, P-selectin and the ESAM-related protein JAM-A. We found that surface expression of each of these proteins was similar on ESAM$^{-/-}$ and wild-type mouse platelets (Table 1). Further, P-selectin expression following platelet activation was similar on ESAM$^{-/-}$ and wild-type platelets, demonstrating normal α-granule secretion in ESAM$^{-/-}$ mice (Table 1).

Calcium mobilization and $\alpha_{IIb}\beta_3$ activation in ESAM$^{-/-}$ platelets

We next examined whether ESAM regulates early platelet signaling events downstream of agonist stimulation by measuring calcium mobilization and $\alpha_{IIb}\beta_3$ activation in ESAM-null platelets. Calcium mobilization in response to either a

Table 1 Wild-type and ESAM$^{-/-}$ platelet surface molecule expression

	Resting		Activated*	
	Wild-type (n = 2)	ESAM$^{-/-}$ (n = 3)	Wild-type (n = 2)	ESAM$^{-/-}$ (n = 3)
$\alpha_{IIb}\beta_3$	236 ± 6	222 ± 12	282.5 ± 24	264 ± 17
GPIbα	145 ± 12	129 ± 17	72.6 ± 18.6	63.3 ± 3.5
JAM-A	28.8 ± 2.4	25.9 ± 1.0	35.1 ± 4.7	37.3 ± 5.0
P-selectin	3.16 ± 0.66	3.92 ± 0.67	52.8 ± 7.8	50.3 ± 1.7

*Platelets were activated with 200 μM AYPGKF. Mean fluorescence intensity (mean ± SEM) for resting and activated platelets is reported.

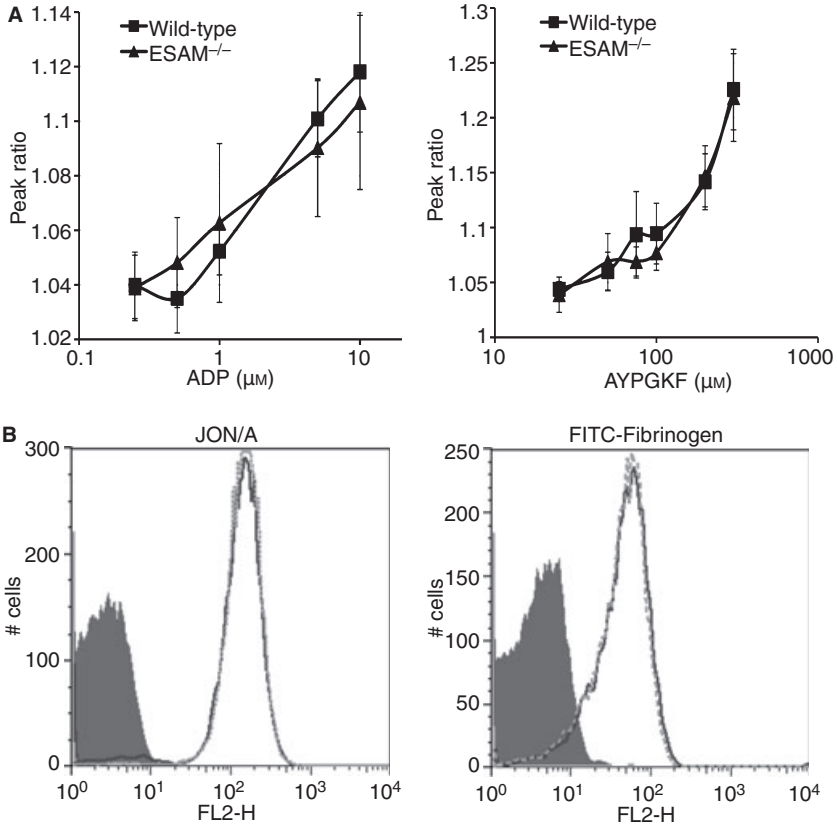

Fig. 5. ESAM does not regulate calcium mobilization or $\alpha_{IIb}\beta_3$ activation in isolated mouse platelets. (A) Calcium mobilization in response to ADP (left panel) and the PAR4 agonist AYPGKF (right panel) were measured using the fluorescent calcium indicator Fura-2 as described in Methods. Values are mean ± SD for two independent experiments. (B) Flow cytometry was used to evaluate $\alpha_{IIb}\beta_3$ activation by stimulating platelets from wild-type and ESAM$^{-/-}$ mice with AYPGQV (500 μM) in the presence of either FITC-fibrinogen (right panel) or phycoerythrin-labeled JON/A antibody (left panel). Solid histogram is resting wild-type platelets, solid line is activated wild-type platelets and the dotted line is activated ESAM$^{-/-}$ platelets. Histograms are representative of three independent experiments.

PAR-4 agonist peptide or ADP was the same in ESAM$^{-/-}$ platelets as in wild-type controls (Fig. 5A). Similarly, integrin activation measured using an antibody (JON/A) that is selective for the active conformation of $\alpha_{IIb}\beta_3$ did not differ between ESAM$^{-/-}$ and wild-type platelets over a range of agonist concentrations (50–500 μM AYPGKF; response to 500 μM AYPGKF is shown in Fig. 5B, left panel). Similar results were obtained using FITC-labeled fibrinogen binding to measure $\alpha_{IIb}\beta_3$ activation (Fig. 5B, right panel). Thus, the gain of function observed in the absence of ESAM in the platelet aggregation and *in vivo* thrombosis assays is not due to either increased Ca^{2+} mobilization or $\alpha_{IIb}\beta_3$ activation.

Platelet spreading and clot retraction in ESAM$^{-/-}$ platelets

As calcium mobilization and integrin activation are unaffected in ESAM-deficient platelets, we next examined platelet spreading and clot retraction as measures of late platelet signaling events in the absence of ESAM. Platelet spreading on immobilized fibrinogen, a process dependent on $\alpha_{IIb}\beta_3$ out-

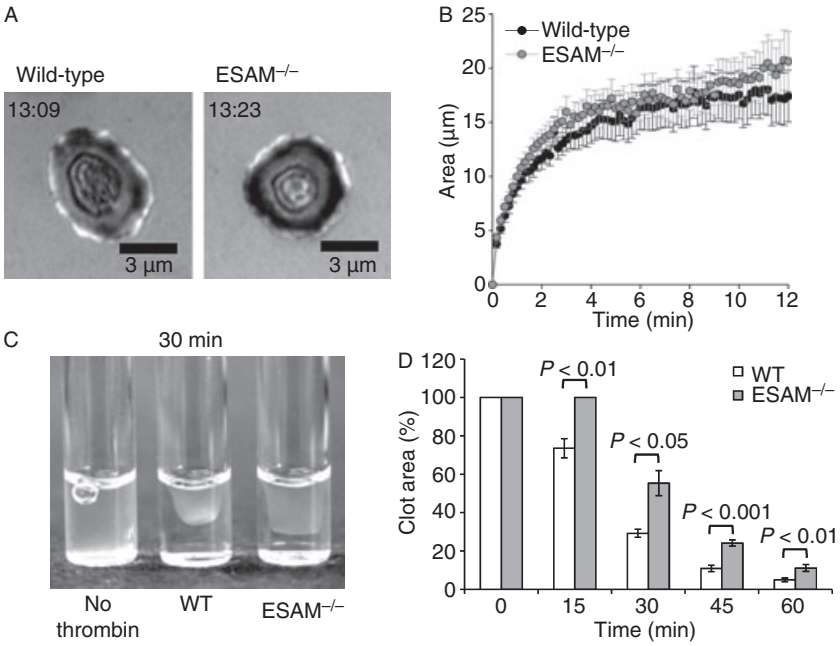

Fig. 6. Clot retraction is delayed in the absence of ESAM. (A, B) Wild-type and ESAM$^{-/-}$ platelets were spread on immobilized fibrinogen in the presence of the PAR-4 agonist AYPGKF (200 μM). The time stamp indicates time after initial contact for the platelet shown. The area (mean ± SEM) of platelets over time in two independent experiments is reported in (B). Black circles represent wild-type and gray circles represent ESAM$^{-/-}$ platelets. (C, D) Clot retraction was induced by adding 10 U mL^{-1} thrombin to either wild-type or ESAM$^{-/-}$ PRP at 37 °C. Image is representative of difference 30 min after the addition of thrombin. Clot retraction was quantified by determining the two-dimensional area occupied by the clot as described in Methods. Values are mean ± SEM for six mice in each group.

side-in signaling, was indistinguishable in the presence and absence of ESAM (Fig. 6A,B). In contrast, we found that fibrin clot retraction following thrombin stimulation is significantly delayed in the absence of ESAM (Fig. 6C,D). Thus, ESAM is dispensable for platelet spreading, but appears to be necessary for efficient clot retraction, an event that involves post-aggregation signaling.

Interactions with the ESAM PDZ ligand domain

Finally, we sought to identify proteins that interact with ESAM's cytoplasmic tail as an alternative approach to determine the molecular mechanism by which ESAM regulates platelet function. The cytoplasmic domain of ESAM terminates in a type-I PDZ domain binding motif that is highly conserved across species (Fig. 7A). The only known partner for ESAM is the PDZ domain containing protein MAGI-1 [15], which we were unable to detect by Western blot in platelets (data not shown). To identify other potential ESAM interacting proteins, we generated a GST fusion protein containing the last 30 amino acid residues of the ESAM cytoplasmic tail, which includes the c-terminal PDZ domain binding motif. This fusion protein was used to probe a protein array containing 96 different PDZ domains from 48 different proteins [22]. We found that GST-ESAM bound to several PDZ domains on the array (Fig. 7B,C). Among the proteins identified as interacting with ESAM on the array, only CAL and NHERF-1 were conclusively determined to be expressed in human platelets by Western blot analysis (Fig. 7D, top panel). An association of ESAM and NHERF-1 was confirmed in both resting and activated platelets by co-immunoprecipitation using anti-ESAM to immunoprecipitate both proteins or by doing the reverse using anti-NHERF-1 as the immunoprecipitating antibody (Fig. 7D, bottom panel). We were unable to demonstrate an association of ESAM and CAL in platelets (data not shown).

Discussion

Increasing evidence suggests that contact-dependent molecular interactions have an important physiological role in the maintenance of thrombus size and stability *in vivo* [24]. A diverse set of platelet surface proteins are involved in these events, including traditional signaling receptors such as G protein coupled receptors and receptor tyrosine kinases, as well as adhesive proteins such as $\alpha_{IIb}\beta_3$. In the present study, we found that ESAM, one of several CTX-family members expressed on platelets, translocates to platelet–platelet contacts following platelet activation, suggesting a role for this protein in post-aggregation platelet functional events as well.

ESAM was originally predicted to be an adhesion molecule, as it can bind to itself homophilically when expressed on adjacent cells [12,14], and it is found at tight junctions of endothelial cells [12]. Our finding that ESAM is localized to platelet–platelet contacts is consistent with these results. To our knowledge this is the first demonstration of a cell surface

A

Species	ESAM c-terminus
H. sapiens	MVPAQSQAGSLV
M. musculus	MVPAQSQAGSLV
B. taurus	MVPAQSQAGSLV
C. l. familiaris	MVPAQSQAGSLV
G. gallus	MVPAQSRAGSLV
D. rerio	MVPAQNQAGSLV

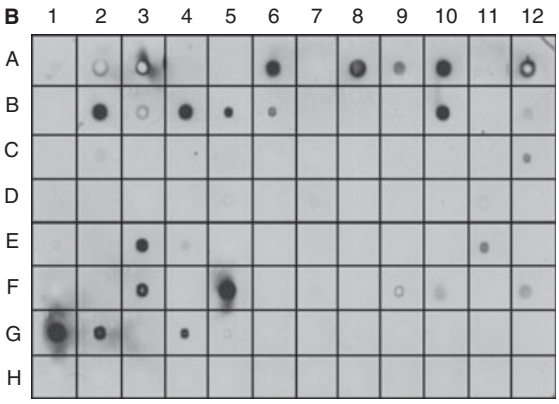

C

List of PDZ domains contained on the array

A1. MAGI-1 PDZ1	C1. INADL PDZ6	E1. RPH2	**G1. PDZK1 PDZ4**
A2. MAGI-1 PDZ2	C2. DLG1 PDZ1/2	E2. Harmonin1	**G2. PDZK2 PDZ1**
A3. MAGI-1 PDZ3	C3. DLG1 PDZ3	**E3. Harmonin2**	G3. PDZK2 PDZ2
A4. MAGI-1 PDZ4/5	C4. DLG3 PDZ1/2	E4. Neurabin	**G4. PDZK2 PDZ3**
A5. MAGI-2 PDZ1	C5. DLG3 PDZ3	E5. Spinophilin	G5. PDZK2 PDZ4
A6. MAGI-2 PDZ2	C6. DLG2 PDZ1/2	E6. A1 syntrophin	G6. LNX1 PDZ1
A7. MAGI-2 PDZ3	C7. DLG2 PDZ3	E7. B1 syntrophin	G7. LNX1 PDZ2
A8. MAGI-2 PDZ4	C8. SIPA1L1	E8. B2 syntrophin	G8. LNX1 PDZ3
A9. MAGI-2 PDZ5	C9. ERBIN	E9. G1 syntrophin	G9. LNX1 PDZ4
A10. MAGI-3 PDZ1	C10. ZO-1 PDZ1	E10. G2 syntrophin	G10. LNX2 PDZ1
A11. MAGI-3 PDZ2	C11. ZO-1 PDZ2	E11. PDZD2	G11. LNX2 PDZ2
A12. MAGI-3 PDZ3	C12. ZO-1 PDZ3	E12. MUPP-1 PDZ1	G12. LNX2 PDZ4
B1. MAGI-3 PDZ4	D1. ZO-2 PDZ1	F1. MUPP-1 PDZ6	H1. PTPN4
B2. MAGI-3 PDZ5	D2. ZO-2 PDZ2	F2. MUPP-1 PDZ7	H2. RhoGEF
B3.NHERF-1 PDZ1	D3. ZO-2 PDZ3	**F3. MUPP-1 PDZ8**	H3. RA-GEF
B4.NHERF-1 PDZ2	D4. ZO-3 PDZ1	F4. MUPP-1 PDZ10	H4. Enigma
B5.NHERF-2 PDZ1	D5. ZO-3 PDZ2	**F5. MUPP-1 PDZ12**	H5. LARG
B6.NHERF-2 PDZ2	D6. ZO-3 PDZ3	F6. MUPP-1 PDZ13	H6. MAST205
B7.PSD95 PDZ1/2	D7. RGS3	F7. PTPN13 PDZ1	H7. PTPN3
B8.PSD95 PDZ3	D8. GIPC	F8. PTPN13 PDZ3	H8. Shank
B9. GEF1	D9. LIN7A	F9. PTPN13 PDZ4/5	H9. Tamalin
B10. CAL	D10. LIN7B	F10. PDZK1 PDZ1	H10. PAR3 PDZ1
B11.nNOS	D11. DENSIN180	F11. PDZK1 PDZ2	H11. PAR3 PDZ2
B12.INADL PDZ5	D12. RPH1	F12. PDZK1 PDZ3	H12. PAR3 PDZ3

D

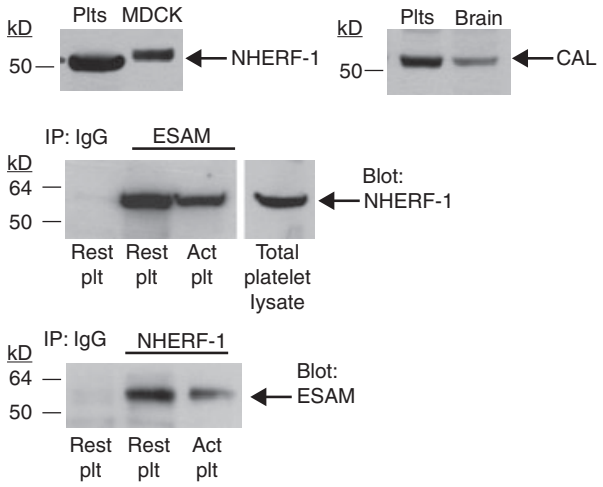

Fig. 7. ESAM associates with the scaffold protein NHERF-1 in human platelets. (A) Amino acid sequence of the ESAM cytoplasmic tail c-terminus in multiple species. The PDZ domain binding motif is underlined. (B) A PDZ domain array was probed using a GST-ESAM cytoplasmic tail fusion protein as described in Methods. There were several positive hits, including PDZ domain 2 of NHERF-1. (C) A complete list of PDZ domains present on the array. Strongly positive hits are in bold. (D) Top panel: Western blot results demonstrating NHERF-1 and CAL expression in human platelets. MDCK cells expressing human NHERF-1 and human brain lysate were used as positive controls. Bottom panel: Co-immunoprecipitation of ESAM and NHERF-1 in human platelets. Human platelet lysates were subjected to immunoprecipitation with anti-ESAM, anti-NHERF-1 or a non-specific IgG control antibody. The membranes were immunoblotted using an anti-NHERF-1 antibody (for ESAM IP) or an anti-ESAM antibody (NHERF-1 IP). Blots are representative of three independent experiments.

molecule concentrating at platelet–platelet contacts, which points to a novel role for ESAM and possibly other CTX-family members in platelet function. Interestingly, we found that platelet aggregates were more stable in the absence of ESAM *in vitro* and thrombi were larger and more stable in ESAM$^{-/-}$ mice *in vivo*. These findings are in agreement with a recent study demonstrating enhanced thrombus formation following morpholino-mediated knockdown of ESAM in zebrafish [18]. In addition, a similar gain of function phenotype is observed in JAM$^{-/-}$ mice [25], suggesting that members of the CTX-family may have overlapping functions in platelets.

Based on the finding that thrombus formation is increased in its absence, ESAM does not appear to contribute adhesive strength to platelet contacts, as might be expected for an adhesion molecule. This conclusion is consistent with recent findings regarding the function of ESAM on endothelial cells. Wegmann *et al.* demonstrated that VEGF-induced vascular permeability is significantly reduced in ESAM-deficient mice [16] (i.e. endothelial cell junctions are more stable in the absence of ESAM). They hypothesized that ESAM has a role in the coordinated disassembly of endothelial cell junctions in order to increase vascular permeability, possibly via effects on the small GTPase Rho. Similarly, Orlova *et al.* recently described an analogous role for the related protein, JAM-C, in the regulation of microvascular permeability via the small GTPase, Rap1 [26]. Taken together, these findings suggest that in both

endothelial cells and platelets ESAM, as well as other CTX-family members, contributes to signaling events that regulate the stability of cell–cell junctions. In endothelial cells, this process is critical in the regulation of both vascular permeability and leukocyte transmigration, while in platelets our data suggest that it is critical in the regulation of thrombus growth and stability.

Despite the increase in aggregation, ESAM-deficient platelets did not have a demonstrable change in cytosolic calcium mobilization or the activation of $\alpha_{IIb}\beta_3$. There are several possible explanations for these findings. First, as ESAM presumably depends on homophilic engagement of molecules on adjacent cells to exert its effects, any potential role in platelet signaling regulating integrin activation may not be apparent in the single cell suspensions in which the calcium and fibrinogen binding studies were performed. Second, given its initial localization in α-granules and subsequent localization at platelet contacts, it is likely that ESAM regulates platelet signaling events following integrin activation and engagement. To address this hypothesis, we examined the role of ESAM in platelet spreading and clot retraction, two functional events that occur following integrin ligand binding. The loss of ESAM has no effect on platelet spreading, although again these studies were performed in the absence of platelet–platelet interactions. In contrast, we found that fibrin clot retraction, a process previously demonstrated to be regulated by contact-dependent signaling events [27], is significantly delayed in the absence of ESAM. It is unclear whether the effect of ESAM on clot retraction is mediated by a signaling pathway related to the one that is responsible for the observed effects on platelet aggregation, or whether these are independent signaling mechanisms both influenced by ESAM.

In this regard, the precise molecular mechanism by which ESAM regulates platelet function remains to be determined. The enhanced aggregation and thrombus formation in the ESAM knockout is reminiscent of the phenotype observed following the genetic deletion or antibody crosslinking of a growing list of platelet surface proteins that are considered negative regulators of platelet function, including PECAM-1 [8], CEACAM1 [9], and G6b-B [28]. However, the ESAM cytoplasmic tail does not contain ITIM domains (or any other phosphorylatable tyrosines), as described for these proteins [28–31], to explain its effects. It does, however, contain other potential protein interaction motifs. The ESAM cytoplasmic tail contains a proline-rich region that could bind SH3 domains and a c-terminal PDZ domain binding motif that is highly conserved across species, which suggests that recruitment of cytoplasmic proteins to the membrane is a likely mechanism by which it exerts its function. Accordingly, we have identified a PDZ domain containing scaffold protein, NHERF-1, that binds to the ESAM cytoplasmic tail *in vitro* and associates with ESAM in platelets. NHERF-1 contains two PDZ domains that interact with a diverse set of proteins, including GPCRs [32], G proteins and PLCβ [33] among others, as well as an ERM-binding domain that mediates interactions with components of the cytoskeleton [34]. Although additional studies are needed to definitively establish a role for NHERF-1 in the function of ESAM, the finding that ESAM accumulates at platelet contacts suggests a mechanism whereby ESAM may recruit NHERF-1 or other as yet unidentified cytoplasmic proteins to sites of platelet–platelet contact in order to regulate one or more key signaling pathways in platelets.

In conclusion, we have described a novel regulatory mechanism for the control of thrombus growth and stability involving the platelet membrane protein ESAM. These findings further advance our knowledge of the dynamic processes involved in platelet plug formation and stabilization, and future studies examining the relationship between ESAM, other CTX-family members and platelet signaling pathways may uncover a broader role for this family of cell adhesion molecules in platelet physiology.

Addendum

T.J. Stalker designed and performed experiments, analyzed data and wrote the paper; J. Wu, A. Morgans, E.A. Traxler, L. Wang, M.S. Chatterjee and D. Lee performed experiments and analyzed data; T. Quertermous, R.A. Hall, D.A. Hammer and S.L. Diamond provided vital analytical tools; L.F. Brass designed experiments, analyzed data and wrote the paper.

Acknowledgements

These studies were supported by grant numbers P01-HL040387 (L.F. Brass) and R33-HL087317 (D.A. Hammer, S.L. Diamond and L.F. Brass) from the National Heart, Lung and Blood Institute. T.J. Stalker was supported by American Heart Association post-doctoral fellowship 0525630U.

Disclosure of Conflict of Interests

The authors state that they have no conflict of interest.

References

1 Law DA, DeGuzman FR, Heiser P, Ministri-Madrid K, Killeen N, Phillips DR. Integrin cytoplasmic tyrosine motif is required for outside-in alphaIIbbeta3 signalling and platelet function. *Nature* 1999; **401**: 808–11.

2 Cosemans JM, Munnix IC, Wetzker R, Heller R, Jackson SP, Heemskerk JW. Continuous signaling via PI3K isoforms beta and gamma is required for platelet ADP receptor function in dynamic thrombus stabilization. *Blood* 2006; **108**: 3045–52.

3 Goto S, Tamura N, Ishida H, Ruggeri ZM. Dependence of platelet thrombus stability on sustained glycoprotein IIb/IIIa activation through adenosine 5′-diphosphate receptor stimulation and cyclic calcium signaling. *J Am Coll Cardiol* 2006; **47**: 155–62.

4 Andre P, Prasad KS, Denis CV, He M, Papalia JM, Hynes RO, Phillips DR, Wagner DD. CD40L stabilizes arterial thrombi by a beta3 integrin–dependent mechanism. *Nat Med* 2002; **8**: 247–52.

5 Angelillo-Scherrer A, Burnier L, Flores N, Savi P, DeMol M, Schaeffer P, Herbert JM, Lemke G, Goff SP, Matsushima GK, Earp HS, Vesin C, Hoylaerts MF, Plaisance S, Collen D, Conway EM, Wehrle-Haller

B, Carmeliet P. Role of Gas6 receptors in platelet signaling during thrombus stabilization and implications for antithrombotic therapy. *J Clin Invest* 2005; **115**: 237–46.
6 Prevost N, Woulfe D, Tanaka T, Brass LF. Interactions between Eph kinases and ephrins provide a mechanism to support platelet aggregation once cell-to-cell contact has occurred. *Proc Natl Acad Sci USA* 2002; **99**: 9219–24.
7 Zhu L, Bergmeier W, Wu J, Jiang H, Stalker TJ, Cieslak M, Fan R, Boumsell L, Kumanogoh A, Kikutani H, Tamagnone L, Wagner DD, Milla ME, Brass LF. Regulated surface expression and shedding support a dual role for semaphorin 4D in platelet responses to vascular injury. *Proc Natl Acad Sci USA* 2007; **104**: 1621–6.
8 Falati S, Patil S, Gross PL, Stapleton M, Merrill-Skoloff G, Barrett NE, Pixton KL, Weiler H, Cooley B, Newman DK, Newman PJ, Furie BC, Furie B, Gibbins JM. Platelet PECAM-1 inhibits thrombus formation in vivo. *Blood* 2006; **107**: 535–41.
9 Wong C, Liu Y, Yip J, Chand R, Wee JL, Oates L, Nieswandt B, Reheman A, Ni H, Beauchemin N, Jackson DE. CEACAM1 negatively regulates platelet–collagen interactions and thrombus growth in vitro and in vivo. *Blood* 2009; **113**: 1818–28, blood-2008-06-165043 [pii] 10.1182/blood-2008-06-165043.
10 Naik UP, Ehrlich YH, Kornecki E. Mechanisms of platelet activation by a stimulatory antibody: cross-linking of a novel platelet receptor for monoclonal antibody F11 with the Fc gamma RII receptor. *Biochem J* 1995; **310** (Pt 1): 155–62.
11 Santoso S, Sachs UJ, Kroll H, Linder M, Ruf A, Preissner KT, Chavakis T. The junctional adhesion molecule 3 (JAM-3) on human platelets is a counterreceptor for the leukocyte integrin Mac-1. *J Exp Med* 2002; **196**: 679–91.
12 Nasdala I, Wolburg-Buchholz K, Wolburg H, Kuhn A, Ebnet K, Brachtendorf G, Samulowitz U, Kuster B, Engelhardt B, Vestweber D, Butz S. A transmembrane tight junction protein selectively expressed on endothelial cells and platelets. *J Biol Chem* 2002; **277**: 16294–303.
13 Kojima H, Kanada H, Shimizu S, Kasama E, Shibuya K, Nakauchi H, Nagasawa T, Shibuya A. CD226 mediates platelet and megakaryocytic cell adhesion to vascular endothelial cells. *J Biol Chem* 2003; **278**: 36748–53.
14 Hirata K, Ishida T, Penta K, Rezaee M, Yang E, Wohlgemuth J, Quertermous T. Cloning of an immunoglobulin family adhesion molecule selectively expressed by endothelial cells. *J Biol Chem* 2001; **276**: 16223–31.
15 Wegmann F, Ebnet K, Du Pasquier L, Vestweber D, Butz S. Endothelial adhesion molecule ESAM binds directly to the multidomain adaptor MAGI-1 and recruits it to cell contacts. *Exp Cell Res* 2004; **300**: 121–33.
16 Wegmann F, Petri B, Khandoga AG, Moser C, Khandoga A, Volkery S, Li H, Nasdala I, Brandau O, Fassler R, Butz S, Krombach F, Vestweber D. ESAM supports neutrophil extravasation, activation of Rho, and VEGF-induced vascular permeability. *J Exp Med* 2006; **203**: 1671–7.
17 Maynard DM, Heijnen HF, Horne MK, White JG, Gahl WA. Proteomic analysis of platelet alpha-granules using mass spectrometry. *J Thromb Haemost* 2007; **5**: 1945–55.
18 O'Connor MN, Salles II, Cvejic A, Watkins NA, Walker A, Garner SF, Jones CI, Macaulay IC, Steward M, Zwaginga JJ, Bray SL, Dudbridge F, De Bono B, Goodall AH, Deckmyn H, Stemple DL, Ouwehand WH. Functional genomics in zebrafish permits rapid characterization of novel platelet membrane proteins. *Blood* 2008; **113**: 4754–62.
19 Ishida T, Kundu RK, Yang E, Hirata K, Ho YD, Quertermous T. Targeted disruption of endothelial cell-selective adhesion molecule inhibits angiogenic processes in vitro and in vivo. *J Biol Chem* 2003; **278**: 34598–604.
20 Woulfe D, Jiang H, Morgans A, Monks R, Birnbaum M, Brass LF. Defects in secretion, aggregation, and thrombus formation in platelets from mice lacking Akt2. *J Clin Invest* 2004; **113**: 441–50.
21 Falati S, Gross P, Merrill-Skoloff G, Furie BC, Furie B. Real-time in vivo imaging of platelets, tissue factor and fibrin during arterial thrombus formation in the mouse. *Nat Med* 2002; **8**: 1175–81.
22 Weiler-Guettler H, Christie PD, Beeler DL, Healy AM, Hancock WW, Rayburn H, Edelberg JM, Rosenberg RD. A targeted point mutation in thrombomodulin generates viable mice with a prethrombiotic state. *J Clin Invest* 1998; **101**: 1983–91.
23 He J, Bellini M, Inuzuka H, Xu J, Xiong Y, Yang X, Castleberry AM, Hall RA. Proteomic analysis of beta1-adrenergic receptor interactions with PDZ scaffold proteins. *J Biol Chem* 2006; **281**: 2820–7.
24 Brass LF, Zhu L, Stalker TJ. Minding the gaps to promote thrombus growth and stability. *J Clin Invest* 2005; **115**: 3385–92, 10.1172/JCI26869.
25 Naik MU, Naik UP. Junctional adhesion molecule-A negatively regulates integrin alpha IIB beta 3-dependent contractile signaling in platelets. *J Thromb Haemost* 2009; **7**: OC-MO-046.
26 Orlova VV, Economopoulou M, Lupu F, Santoso S, Chavakis T. Junctional adhesion molecule-C regulates vascular endothelial permeability by modulating VE-cadherin-mediated cell–cell contacts. *J Exp Med* 2006; **203**: 2703–14.
27 Prevost N, Woulfe DS, Jiang H, Stalker TJ, Marchese P, Ruggeri ZM, Brass LF. Eph kinases and ephrins support thrombus growth and stability by regulating integrin outside-in signaling in platelets. *Proc Natl Acad Sci USA* 2005; **102**: 9820–5.
28 Newland SA, Macaulay IC, Floto AR, De Vet EC, Ouwehand WH, Watkins NA, Lyons PA, Campbell DR. The novel inhibitory receptor G6B is expressed on the surface of platelets and attenuates platelet function in vitro. *Blood* 2007; **109**: 4806–9.
29 Cicmil M, Thomas JM, Leduc M, Bon C, Gibbins JM. Platelet endothelial cell adhesion molecule-1 signaling inhibits the activation of human platelets. *Blood* 2002; **99**: 137–44.
30 Wong C, Liu Y, Yip J, Chand R, Wee JL, Oates L, Nieswandt B, Reheman A, Ni H, Beauchemin N, Jackson DE. CEACAM1 negatively regulates platelet–collagen interactions and thrombus growth in vitro and in vivo. *Blood* 2008; **113**: 1818–28, blood-2008-06-165043 [pii] 10.1182/blood-2008-06-165043.
31 Mori J, Pearce AC, Spalton JC, Grygielska B, Eble JA, Tomlinson MG, Senis YA, Watson SP. G6b-B inhibits constitutive and agonist-induced signaling by glycoprotein VI and CLEC-2. *J Biol Chem* 2008; **283**: 35419–27, M806895200 [pii], 10.1074/jbc.M806895200.
32 Hall RA, Ostedgaard LS, Premont RT, Blitzer JT, Rahman N, Welsh MJ, Lefkowitz RJ. A C-terminal motif found in the beta2-adrenergic receptor, P2Y1 receptor and cystic fibrosis transmembrane conductance regulator determines binding to the Na+/H+ exchanger regulatory factor family of PDZ proteins. *Proc Natl Acad Sci USA* 1998; **95**: 8496–501.
33 Rochdi MD, Watier V, La Madeleine C, Nakata H, Kozasa T, Parent JL. Regulation of GTP-binding protein alpha q (Galpha q) signaling by the ezrin-radixin-moesin-binding phosphoprotein-50 (EBP50). *J Biol Chem* 2002; **277**: 40751–9.
34 Shenolikar S, Voltz JW, Cunningham R, Weinman EJ. Regulation of ion transport by the NHERF family of PDZ proteins. *Physiology (Bethesda)* 2004; **19**: 362–9.